LIMIT STRESS FOR GRANULAR COMPOSITES REINFORCED WITH CONTINUOUS FILAMENTS

By Radoslaw L. Michalowski,[1] Member, ASCE

ABSTRACT: The concept of using continuous filaments (threads) to reinforce soils has been applied in practice for more than a decade. The design of soil structures reinforced with continuous thread is based on limit state techniques where the failure criterion of the composite is the essential function. This paper is focused on deriving such a function. A homogenization technique is used to calculate the components of the macroscopic stress state at failure. The limit condition is anisotropic because of the preferred plane of the filament deposition. In the stress space used here the limit condition has the shape of a convex cone with a cross section close to that of a circle. The numerically derived function gives reasonable estimates of the increase in strength (apparent cohesion) of granular materials reinforced with continuous threads. Further work needs to concentrate on a more accurate description of the stress mobilization in filaments during failure, and on including the filament-matrix slip. The numerically calculated failure criterion has a form convenient for use in stability analyses of structures.

INTRODUCTION

Composites with granular matrices have found extensive application as construction materials in geotechnical engineering, yet little attention has been paid to their modeling. The design of structures with granular matrix composites is predominantly based on limit state analysis, and an accurate description of the macroscopic stress state at failure is particularly needed for realistic design. A substantial body of literature exists on soils reinforced with long metallic strips (of length comparable with the size of the structure), or large sheets of synthetic fabric or geogrid. This type of reinforcement is analyzed using a structural approach where the soil (granular matrix) and reinforcement are considered as two separate structural components. This paper describes a different composite, where it is more appropriate to describe its average (macroscopic) properties before analyzing its structural stability.

The composite considered here has a granular matrix (sand), and is reinforced with very thin continuous filaments (threads) in the amount of about 0.1–0.2% by weight. The linear density of the filament is measured in dtex units (10 dtex = 1 tex = 1 g/km). Each thread consists of a number of monofilaments (not twisted) and, for instance, designation 167/30 describes a thread of density 16.7 g/km with 30 monofilaments in it. The length of the thread in 1 m^3 of the composite is typically more than 100 km and can reach several hundred km/m^3.

Construction with continuous filament composites involves simultaneous deposition of soil slurry and filaments. The result is an anisotropic composite with a preferred plane of filament orientation (bedding plane).

There have been a few attempts at theoretically describing the elastic and elastoplastic properties of thread-reinforced soils (Villard and Jouve 1989; di Prisco and Nova 1993). Results from experimental testing are also available (Leflaive and Liausu 1986; di Prisco and Nova 1993; Sanvito 1995; Stauffer and Holtz 1995). These will be helpful in validating the description presented here. This paper is focused on the macroscopic failure stress (failure criterion) of thread-reinforced granular soils. Stresses at the instant of failure will be homogenized using a technique developed earlier for isotropic fiber-reinforced soils (Michalowski and Zhao 1996a); this technique will now be extended to the anisotropic distribution of reinforcement orientation. Homogenization techniques of a similar type were considered earlier for metal matrix and cementitious composites [for instance, Hill (1964), Budiansky (1965), Shu and Rosen (1967), McLaughlin and Batterman (1970)], and an excellent survey of these techniques can be found in Hashin (1983).

The composite material considered is described in the next section, followed by a brief description of the homogenization concept. Subsequently, the failure criterion for the anisotropic composite will be derived in terms of macroscopic stresses, and a comparison with available laboratory test results will be shown. The paper ends with remarks on limitations of the model.

COMPOSITE MATERIAL REINFORCED WITH CONTINUOUS THREAD

Unlike in metal-based composites, where the matrix material can be considered a continuum, the size of the fibers or filaments, relative to the grain size, plays an important role in determining the type of interaction in granular composites.

Matrix-Filament Interaction

If the diameter of the fiber is an order of magnitude smaller than the grain size, the flexible fiber may be accommodated (in a three-dimensional grain assembly) entirely by the pore space even if the fiber aspect ratio is large. In such a case little or no load can be transferred to the fibers, since the fibers will slip in the process of matrix deformation. However, fibers become effective when the grain size becomes small compared to the fiber diameter [Fig. 1(a)]. In the latter case the number of fiber-grains contact points becomes large enough for the fiber-matrix interface to be considered as continuous and frictional. In the former case the reinforcement will become effective only if it is a continuous and flexible filament so that the force in the filament can be induced due to the "belt friction effect," since the filament will be "wrapped" around the grains or around clusters of grains [Fig. 1(b)]. The nature of the load transfer is then quite different in the two cases shown in Fig. 1.

The belt friction effect is illustrated in Fig. 2. If the filament moves in the direction opposite to force T_1, then force T_2 is equal to

$$T_2 = T_1 e^{\mu\beta} \tag{1}$$

where μ = coefficient of friction between the grains and the filament; and β = envelope (wrap) angle, equal here to $\beta_1 + \beta_2$. The force in the filaments is induced because of the de-

[1]Assoc. Prof., Dept. of Civ. Engrg., The Johns Hopkins Univ., Baltimore, MD 21218.

Note. Associate Editor: Robert Y. Liang. Discussion open until January 1, 1998. To extend the closing date one month, a written request must be filed with the ASCE Manager of Journals. The manuscript for this paper was submitted for review and possible publication on October 28, 1996. This paper is part of the *Journal of Engineering Mechanics*, Vol. 123, No. 8, August, 1997. ©ASCE, ISSN 0733-9399/97/0008-0852–0859/$4.00 + $.50 per page. Paper No. 14408.

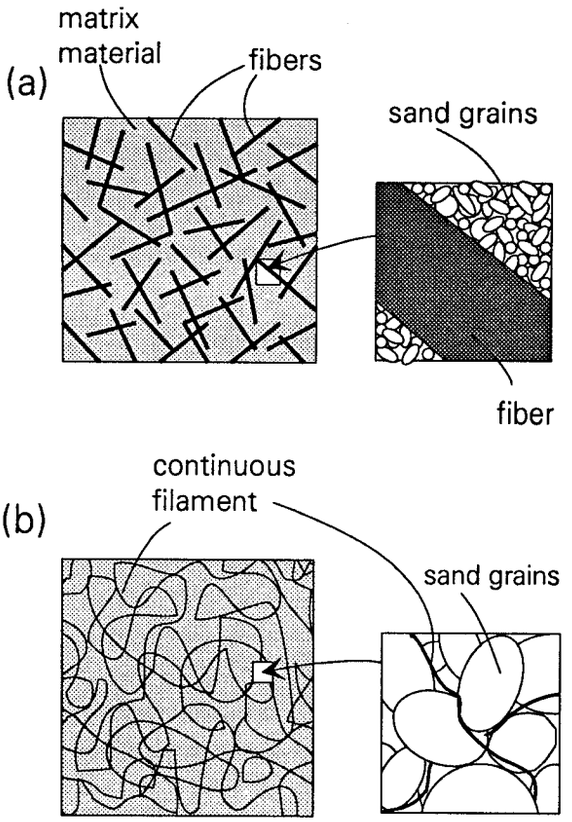

FIG. 1. Reinforced Soil: (a) Fiber Reinforcement; (b) Continuous Thin Filament

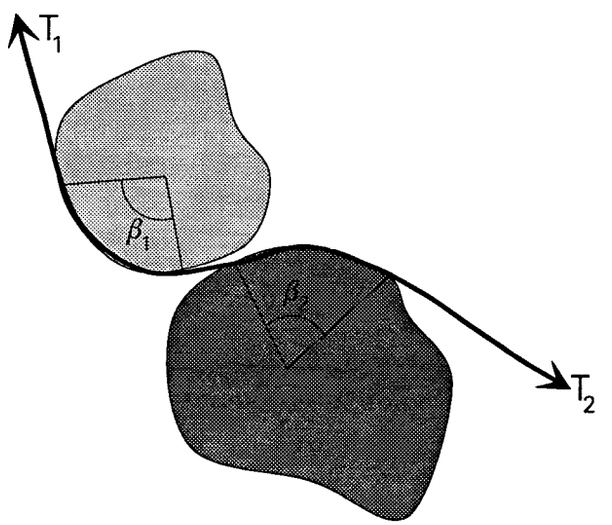

FIG. 2. Filament Wrapped around Clusters of Grains

formation of the matrix. A tensile force so induced will not relax due to slippage because of the "serpentine" deposition of the filaments in the matrix. However, during a deformation process only a portion of the filaments is subjected to extension (stretching), whereas the remaining part is likely to kink because of the inability of filaments to carry compression (also, portions of filaments at transition from the extension to the compression regime may slip). It is the portion of the filaments subjected to extension that will contribute foremost to the composite strength.

Filament Distribution

Two functions convenient for description of the axisymmetrical distribution of the filament orientation are considered in this subsection.

The distribution of the filaments in the granular composite is deemed to be anisotropic because of the techniques used for its deposition. The bedding (deposition) plane is the preferred plane of filament orientation. The distribution of the threads is then likely to be axisymmetrical with respect to the axis perpendicular to the deposition plane.

The average density of the filament distribution is defined as

$$\bar{\rho} = \frac{V_f}{V} \tag{2}$$

where V_f = volume of the filaments; and V = total volume of the specimen. The distribution of orientation of the filaments can be described as the distribution of the filament concentration $\rho(\theta)$ (volumetric density), similar to the distribution of orientation of fibers in fiber-reinforced composites. The fraction of the filaments contained in volume dV in Fig. 3(a) is understood here as the portion whose tangents are parallel to the radii contained within volume dV. Referring to the xOz plane in Fig. 3(a) as the bedding plane, the density of the filament distribution (axisymmetric about y) can be described as

$$\rho(\theta) = \rho_{min} + a|\cos^n\theta| \tag{3}$$

where ρ_{min} = minimum density (volumetric concentration); n = parameter indicating anisotropy of distribution (zero if isotropic); and a = difference between the maximum and minimum $\rho(\theta)$. A more convenient set of parameters may include a ratio b of minimum to maximum of $\rho(\theta)$, and the average filament concentration $\bar{\rho}$. Referring to Fig. 3(a), the average volumetric concentration for an anisotropic composite is

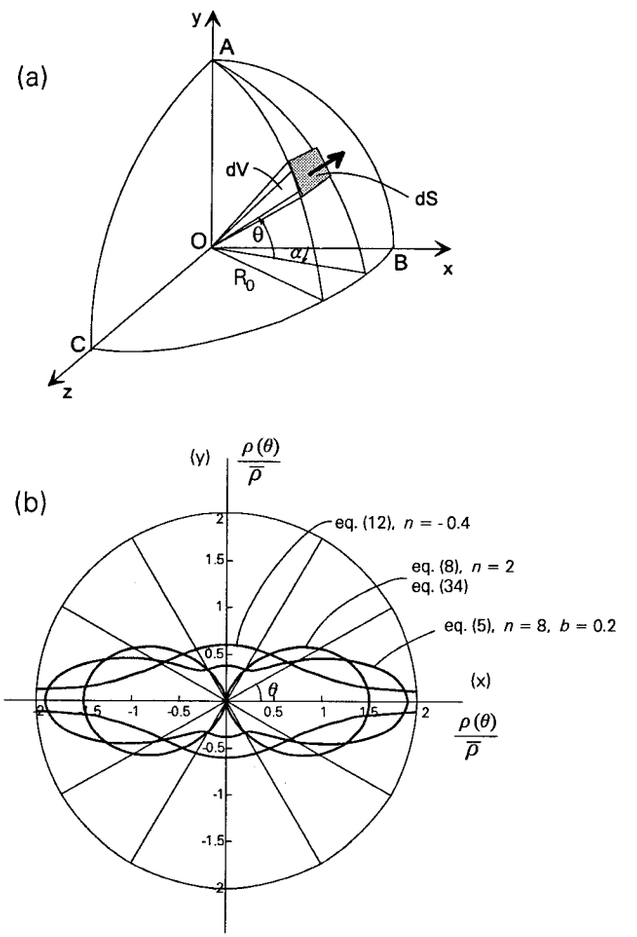

FIG. 3. Filament Concentration $\rho(\theta)$: (a) Integration Space; (b) Polar Plot of Different Filament Orientation Distributions

$$\bar{\rho} = \frac{1}{V}\int_V \rho(\theta)\, dV = \frac{6}{\pi R_0^3}\int_0^{\pi/2}\int_0^{\pi/2} \rho(\theta)\,\frac{1}{3}R_0^3 \cos\theta\, d\alpha\, d\theta \quad (4)$$

The expression in (4) can be used to arrive at a different form of the filament concentration function given in (3)

$$\rho(\theta) = \bar{\rho}B\left(\frac{b}{1-b} + |\cos^n\theta|\right) \quad (5)$$

where $b = \rho_{min}/\rho_{max}$, and

$$B = \frac{1}{\dfrac{b}{1-b} + \displaystyle\int_0^{\pi/2} \cos^{(1+n)}\theta\, d\theta} \quad (6)$$

Examples of the distribution in (5) are shown in the polar plot in Fig. 3(b). The integral in the denominator of (6) does not have a convenient closed form for a general case of n. When the exponent n is a positive even integer, coefficient B in (6) becomes

$$B = \frac{1}{\dfrac{b}{1-b} + \dfrac{n!!}{(1+n)!!}} \quad (7)$$

where !! = double factorial [$n!! = 2\cdot4\cdot6 \ldots n$ and $(n+1)!! = 3\cdot5\cdot7 \ldots (n+1)$]. For a realistic case where no filament has a tangent perpendicular to the bedding plane ($b = 0$), a convenient form of the concentration function results (for even natural n)

$$\rho(\theta) = \bar{\rho}\,\frac{(1+n)!!}{n!!}\cos^n\theta \quad (8)$$

The expressions in (5) and (8) describe the distribution of filament orientation as a function of inclination angle θ to the bedding plane (axisymmetrical distribution about axis y in Fig. 3). An example of distribution in (8) with $n = 2$ is presented in Fig. 3(b). The polar plot of $\rho(\theta)$ in Fig. 3(b) becomes more "flat" with an increase in n.

A distribution function similar to that in (3) (but with the sine function) can be used for fiber (or filament) composites with a preferred direction of fiber orientation (rather than a plane)

$$\rho(\theta) = \rho_{min} + a|\sin^n\theta| \quad (9)$$

or

$$\rho(\theta) = \bar{\rho}B\left(\frac{b}{1-b} + |\sin^n\theta|\right) \quad (10)$$

where

$$B = (1-b)\,\frac{1+n}{1+bn} \quad (11)$$

When no filament is expected in the plane transverse to the preferred direction ($b = \rho_{min}/\rho_{max} = 0$), the distribution function in (10) assumes a convenient form

$$\rho(\theta) = \bar{\rho}(1+n)|\sin^n\theta| \quad (12)$$

This function is characteristic of composites with fiber (filament) orientation concentrated about a preferred direction. However, it can be employed also for the description of filament distribution with a preferred plane when negative n is used [Fig. 3(b)].

HOMOGENIZATION

A homogenization technique is used here to find the average stresses in the composite at failure (failure condition). Failure is defined as the point on the stress-strain curve associated with zero stiffness. The rate of change of elastic energy is zero at failure, and the rate of work of external load must be equal to the work dissipation rate in the composite. Viscous effects are not considered here, and the work dissipation is attributed to plastic deformation.

An increment of macroscopically homogeneous deformation of the composite element at failure is considered with the average (macroscopic) stresses $\bar{\sigma}_{ij}$ and strain rate $\dot{\bar{\varepsilon}}_{ij}$. The rate of work of the average stress is equal to the rate of work dissipation per unit volume

$$\bar{\sigma}_{ij}\dot{\bar{\varepsilon}}_{ij} = \frac{1}{V}\int_V \dot{D}(\dot{\varepsilon}_{ij})\, dV \quad (13)$$

The formula in (13) will be used to find the components of the macroscopic stress tensor at failure. A plane-stain deformation increment will be considered although the composite structure is three-dimensional. A similar technique was used earlier for deriving a failure criterion for an isotropic fiber-reinforced granular-matrix composite (Michalowski and Zhao 1996a). Here the anisotropy of the distribution of filament concentration makes the application of this technique more elaborate, but still tractable, and it is presented in the next section.

MACROSCOPIC FAILURE STRESS

A representative composite element in Fig. 4(a) is subjected to plane-strain deformation as shown in Fig. 4(b). The matrix of the composite conforms to the classical Mohr-Coulomb failure criterion; its deformation at failure is assumed to be equal to the macroscopic deformation, and it is governed by the normality rule. The dilatancy of the composite is assumed here to conform to that of the matrix. Under plane-strain conditions ($\dot{\varepsilon}_2 = \dot{\varepsilon}_z = 0$) the associative flow rule leads to the following relation for the deformation components:

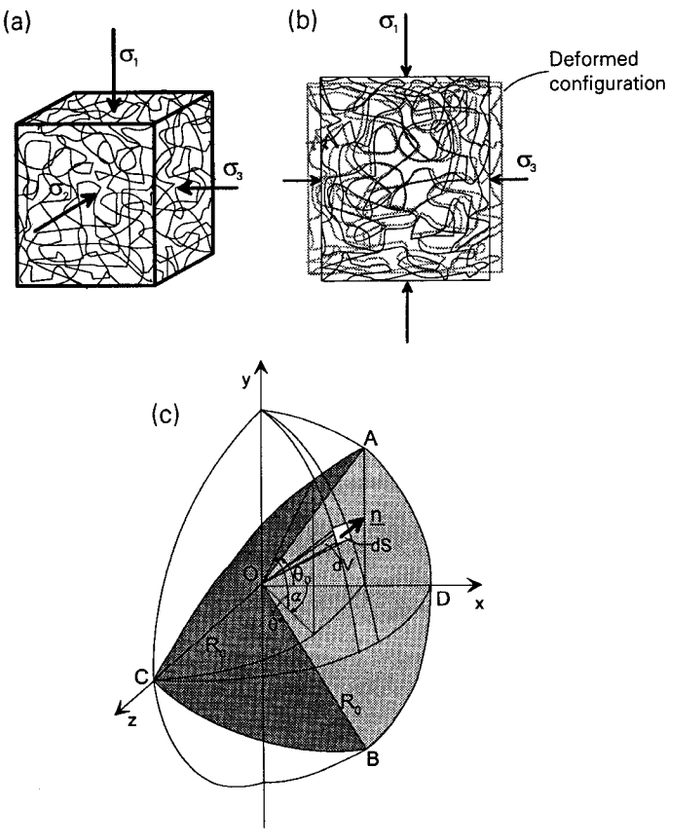

FIG. 4. Continuous Filament-Reinforced Composite: (a) Three-Dimensional Element; (b) Plane-Strain Deformation of Composite Element; (c) Quarter-Spherical Integration Surface

$$\frac{\dot{\varepsilon}_v}{\dot{\gamma}_{max}} = \frac{\dot{\varepsilon}_1 + \dot{\varepsilon}_3}{\dot{\varepsilon}_1 - \dot{\varepsilon}_3} = -\sin\varphi \tag{14}$$

and the ratio of the principal strain rates becomes

$$\frac{\dot{\varepsilon}_3}{\dot{\varepsilon}_1} = -\tan^2\left(\frac{\pi}{4} + \frac{\varphi}{2}\right) = -K_p \tag{15}$$

where φ = angle of internal friction of the matrix material.

Calculations of the work dissipation rate $\dot{D}(\dot{\varepsilon}_{ij})$ in (13) and the derivation of the failure criterion is presented in the following two subsections.

Work Dissipation Rate during Failure

The work dissipation rate in the granular matrix is zero when its deformation is governed by the normality rule (Davis 1968), so the entire dissipation rate is that due to the filaments. To derive the failure criterion we assume that the filaments are rigid-plastic; the consequences of this assumption will be discussed in the section on the comparison of the model and experimental results. Depending on the inclination of the filaments, relative to the principal axes of deformation, the portions of the filaments subjected to extension will reach the yield stress σ_0, whereas the remaining part will kink (or slack) due to the inability of filaments' to support compression. Therefore, the portion subjected to compression needs to be excluded from calculations of the work dissipation rate. The right-hand side of the formula in (13) can be written as

$$\dot{D}(\dot{\varepsilon}_{ij}) = \frac{1}{V}\int_V \rho(\theta)\sigma_0\langle\dot{\varepsilon}_\theta\rangle\, dV \tag{16}$$

where $\rho(\theta)$ = distribution of the volumetric concentration of the filaments, for instance the one expressed in (8); σ_0 = yield stress of the filament material; and $\langle\dot{\varepsilon}_\theta\rangle$ = strain rate in the direction inclined at angle θ to the xz-plane (tension is taken here as negative)

$$\langle\dot{\varepsilon}_\theta\rangle = \begin{cases} |\dot{\varepsilon}_\theta| & \text{if } \dot{\varepsilon}_\theta < 0 \\ 0 & \text{otherwise} \end{cases} \tag{17}$$

Since the strain rate is assumed to be uniform in the representative volume V [linear velocity field in the deformation process in Fig. 4(b)], the dissipation rate in any segment of the filament depends only on its orientation and not on its location in that element. Therefore, for reasons of tractability of the integration process, the representative composite element is transformed into a quarter-spherical shape [Fig. 4(c)] with straight filament segments originating from the center at point O.

The velocity field in the representative composite element, which conforms to the assumed uniform deformation in Fig. 4(b), is

$$\mathbf{v} = -\dot{\varepsilon}_1 x\mathbf{i} - \dot{\varepsilon}_3 y\mathbf{j} \tag{18}$$

A unit vector normal to the surface in Fig. 4(c) is

$$\mathbf{n} = \frac{x}{R_0}\mathbf{i} + \frac{y}{R_0}\mathbf{j} + \frac{z}{R_0}\mathbf{k} \tag{19}$$

where R_0 = radius of the sphere. The strain rate in the direction of the filament identified by coordinates x and y on the spherical surface of the representative element is

$$\dot{\varepsilon}_\theta = -\frac{\mathbf{v}\cdot\mathbf{n}}{R_0} = \frac{\dot{\varepsilon}_1 x^2 + \dot{\varepsilon}_3 y^2}{R_0^2} \tag{20}$$

Considering that $dV = R_0 dS/3$[dS being the surface element; see Fig. 4(c)], (16) can be rewritten as

$$\dot{D}(\dot{\varepsilon}_{ij}) = \frac{\sigma_0}{\pi R_0^4}\int_S \rho(\theta)(-\dot{\varepsilon}_3 x^2 - \dot{\varepsilon}_1 y^2)\, dS \tag{21}$$

where the integration surface S relates only to the part of the spherical surface associated with extension in the radial direction [notice the change of sign because of the definition of positive $\langle\dot{\varepsilon}_\theta\rangle$ in (17)].

The inclination of the filament with respect to the principal directions of the strain rate determines whether it is going to contribute to the composite strength through its tensile strength or is going to kink. The sections of the filaments subjected to extension in the idealized specimen in Fig. 4(c) are separated from the ones under compression by two planes within which the strain rate $\dot{\varepsilon}_\theta = 0$. Denoting angle θ (in plane x, y) associated with the zero extension planes as θ_0, one can write the expression

$$\dot{\varepsilon}_{\theta_0} = \dot{\varepsilon}_1 \sin^2\theta_0 + \dot{\varepsilon}_3 \cos^2\theta_0 = 0 \tag{22}$$

Eqs. (22) and (15) lead to the inclination angle of the two planes containing zero extension filament segments

$$\theta_0 = \pm\left(\frac{\pi}{4} + \frac{\varphi}{2}\right) \tag{23}$$

Now the surface integral in (21) can be written as an integral over the range of α and θ where the filaments are subjected to extension [between planes ACO and BCO in Fig. 4(c)], ignoring the sections of the filaments that are likely to kink (see Appendix I for details)

$$\dot{D}(\dot{\varepsilon}_{ij}) = \frac{1}{\pi}\sigma_0\dot{\varepsilon}_1\int_0^{\pi/2}\int_{-\theta^*}^{\theta^*}\rho(\theta)(K_p\cos^2\alpha\cos^2\theta - \sin^2\theta)\cos\theta\, d\theta\, d\alpha \tag{24}$$

The work dissipation rate in (24) is dependent on the distribution of orientation of the filament concentration $\rho(\theta)$. In the following subsection the failure criterion will be derived with the filament concentration distribution expressed in (5).

Failure Condition

The suggested homogenization scheme in (13) is straightforward when used for isotropic materials (Michalowski and Zhao 1996a), but it becomes more complex when applied to an anisotropic composite. It is convenient, for plane-strain conditions, to represent the failure criterion as the function

$$R - F(p, \psi) = 0 \tag{25}$$

where R and p = in-plane invariants of the macroscopic stress state

$$R\sqrt{\frac{(\bar{\sigma}_x - \bar{\sigma}_y)^2}{4} + \bar{\tau}_{xy}^2}, \quad p = \frac{\bar{\sigma}_1 + \bar{\sigma}_2}{2} \tag{26a,b}$$

and ψ = angle of inclination of the major principal stress to the x-axis. In an incipient deformation process of the element in Fig. 5 the principal directions of the strain rate tensor coincide with axes x' and y'. However, the composite material here is anisotropic, thus the principal directions of the macroscopic stress tensor will, in general, deviate from the principal directions of the strain rate. The equation in (13) can, for the element in Fig. 5, be written as

$$\bar{\sigma}_{x'}\dot{\varepsilon}_{x'} + \bar{\sigma}_{y'}\dot{\varepsilon}_{y'} + 2\bar{\tau}_{x'y'}\dot{\varepsilon}_{x'y'} = \dot{D}(\dot{\varepsilon}_{ij}) \tag{27}$$

We now introduce stress parameter q'

$$q' = \frac{\bar{\sigma}_{x'} - \bar{\sigma}_{y'}}{2} = R\cos 2\psi' \tag{28}$$

where ψ' = angle of inclination of the major principal stress

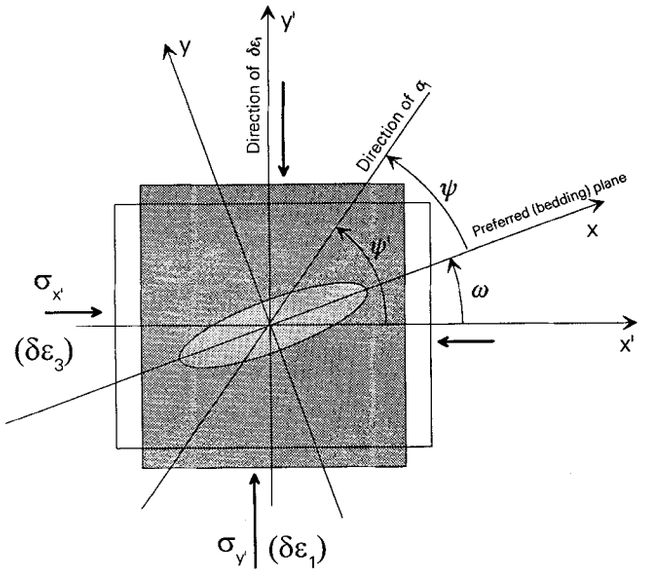

FIG. 5. Plane-Strain Deformation Pattern Used in Homogenization Procedure of Anisotropic Composite

to the x'-axis. Recalling the definition of invariant p in (26) one obtains $\sigma_{x'} = p - q'$ and $\sigma_{y'} = p + q'$, and, noting that $\dot{\varepsilon}_{x'y'} = 0$ (Fig. 5), the expression in (27) takes the following form:

$$q'(\dot{\varepsilon}_1 - \dot{\varepsilon}_3) + p(\dot{\varepsilon}_1 + \dot{\varepsilon}_3) = \dot{D}(\dot{\varepsilon}_{ij}) \tag{29}$$

Coordinate system x', y' is not related to the axes of anisotropy (orientation of the bedding plane), whereas the failure criterion must be derived in reference to the anisotropy pattern. The plane of preferred filament orientation (bedding plane) is assumed here to be perpendicular to the plane of deformation, and its trace in Fig. 5 is marked by the x-axis.

Considering that the Mohr-Coulomb failure criterion used to describe the granular matrix is independent of the intermediate principal stress, the failure criterion for the composite is also expected to be independent of σ_z. The failure criterion then will depend on three independent stress components $\bar{\sigma}_x$, $\bar{\sigma}_y$ and $\bar{\tau}_{xy}$, with direction x uniquely related to the bedding plane (anisotropy pattern). Consequently, (29) can be used to calculate one of the stress components, while the other two are given. However, it was found more convenient to introduce parameters R, p, and ψ instead [see (26)], and calculate the maximum shear stress R for given in-plane average stress p and angle of inclination of the major principal stress ψ. Because of the anisotropy of the composite, this scheme is not straightforward. The following paragraphs describe the procedure used in calculations.

To find the failure criterion in stress space R, p, $\bar{\tau}_{xy}$ (Fig. 6), calculations of R were performed for a constant p and varied inclination angle ψ of the major principal stress to the x-axis. This makes it possible to trace the contour of the failure criterion in plane p = constant. The direction of x describes the anisotropy of the composite (x is the trace of the bedding plane on the plane of deformation).

The principal directions of the strain rate field are kept constant (x', y'; see Fig. 5), and they do not coincide with the principal stress directions since the composite is anisotropic. The problem to be solved is formulated as follows (Fig. 5): given the principal directions of the stress tensor (ψ), what would the preferred plane of filament orientation (ω) need to be in order for the principal directions of strain to be x' and y'? Angle ω is a "deviation" angle defined here as an angle between axes x' and x (the x-axis coincides with the preferred plane of filament orientation).

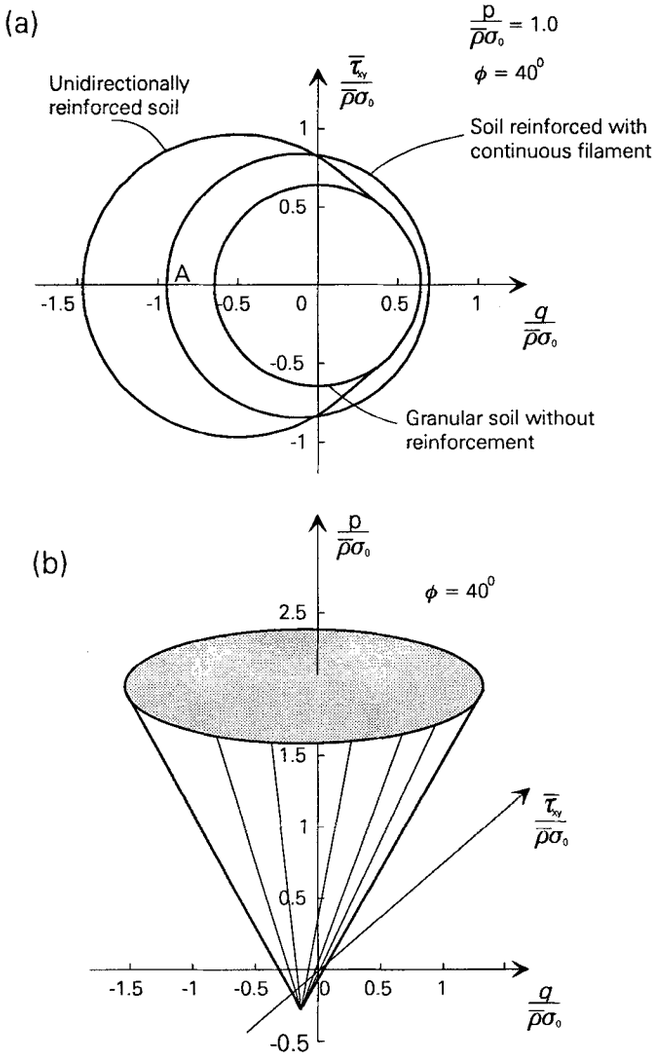

FIG. 6. Strength of Filament-Reinforced Sand: (a) Cross Sections of Failure Criteria; (b) Failure Surface for Sand Reinforced with Continuous Threads in Macroscopic Stress Space

The approach in (29) is analogous to the application of the upper bound theorem of limit analysis. Therefore, the deviation angle (ω) needs to satisfy the requirement that the calculated magnitude of R is a minimum.

Since R is an in-plane stress invariant we can write

$$R = \frac{q}{\cos 2\psi} = \frac{q'}{\cos 2\psi'} = \frac{q'}{\cos 2(\psi + \omega)} \tag{30}$$

and

$$q' = q\frac{\cos 2(\psi + \omega)}{\cos 2\psi} \tag{31}$$

and, from (29) and (15)

$$R = \left(\frac{\dot{D}(\dot{\varepsilon}_{ij})}{\dot{\varepsilon}_1}\frac{1 - \sin\varphi}{2} + p\sin\varphi\right)\frac{1}{\cos 2(\psi + \omega)} \tag{32}$$

With a nonzero deviation angle ω and the distribution of the filament orientation given in (5), the expression for the work dissipation rate in (24), which is to be used in (32), becomes

$$D(\dot{\varepsilon}_{ij}) = \frac{1}{\pi}\sigma_0\dot{\varepsilon}_1\bar{\rho}B\int_0^{\pi/2}\int_{-\theta^*}^{\theta^*}\left(\frac{b}{1-b} + |\cos^n(\theta - \omega^*)|\right)$$
$$\cdot(K_p\cos^2\alpha\cos^2\theta - \sin^2\theta)\cos\theta\, d\theta\, d\alpha \tag{33}$$

where angle ω^* = a function of α and the deviation angle in the plane of deformation ω ($\tan \omega^* = \cos \alpha \tan \omega$). An optimization procedure was used in which the deviation angle ω was varied in (32) and (33), and the minimum of R was sought (for given p and ψ).

The trace of the failure criterion in plane $p/\bar{\rho}\sigma_0 = 1.0$ is illustrated in Fig. 6(a), whereas Fig. 6(b) presents the macroscopic failure condition in space q, p, $\bar{\tau}_{xy}$. For comparison, the cross sections of the failure criterion for the unreinforced sand (matrix) and for the unidirectionally reinforced sand (Michalowski and Zhao 1995, 1996b) are also shown in Fig. 6(a). The distribution of the filaments was considered here in form (8) with $n = 2$, and the cross section of the strength criterion is essentially circular (but off-center). Its shape becomes more elliptical for larger values of exponent n. In the stress space q, p, $\bar{\tau}_{xy}$, the failure criterion for the thread-reinforced soil has the shape of a cone, with its axis shifted with respect to axis p because of the anisotropic properties of the composite [Fig. 6(b)].

COMPARISON TO EXPERIMENTAL RESULTS

This paper is focused on deriving the failure criterion for soils reinforced with continuous filaments. Here the results are compared to those from experimental tests available in the literature (Leflaive and Liausu 1986; di Prisco and Nova 1993; Stauffer and Holtz 1995; Sanvito 1995). All of the results selected for comparison come from triaxial tests on cylindrical specimens. In soil mechanics terminology these results are referred to as drained triaxial compression tests. The specimens were prepared by pluviating sand and simultaneously depositing the filaments in the molds, or by first mixing the composite and then tamping it in the molds. In either case the bedding plane is horizontal (circular cross section of the cylindrical specimen). Therefore, the specimens had an anisotropic distribution of filament orientation, and even more so at the instant of failure, because of the deformation that occurs prior to specimen collapse.

Measurements of the true distribution of the filament orientation in a specimen is a complex task and such measurements are not available. For lack of better data, the distribution in (8) is adopted with $n = 2$

$$\rho(\theta) = \frac{3}{2}\,\bar{\rho}\,\cos^2\theta \tag{34}$$

The polar plot of this distribution is shown in Fig. 3(b).

In all the tests the bedding plane is inclined at $\pi/2$ to the direction of the larger principal stress, thus only one point on the failure surface [point A in Fig. 6(a)] can be validated. Results of tests on filament-reinforced composites performed in a direct shear device (Khay et al. 1990) do not allow for a clear interpretation of the stress state, and, while useful in approximate design, they are not used here for validation of the analytical model.

The model was derived considering the plane-strain deformation process. However, the experimental results available are from tests on specimens subjected to the axisymmetrical stress state. The matrix of the composite was described with the classical Mohr-Coulomb yield condition, which is independent of the intermediate principal stress and includes axisymmetrical stress states. Since true granular soils do not adhere exactly to the Mohr-Coulomb criterion, the properties of the matrix (φ) taken to predict the strength of the triaxial specimens should also be determined from triaxial tests (and they were).

An important difference in the derivation of the failure criterion and the true behavior of the filament-reinforced composite is that stress in the filaments in the extension regime was considered in the derivation to have reached the yield limit σ_0, whereas the filament stress in experiments appeared to be well below rupture. This difference is due to the assumption of the rigid–perfectly plastic deformation process in both the matrix and the filaments. Therefore, when this model is used to predict the strength of the composite, the mobilized stress in the filaments needs to be estimated and used instead of the yield stress σ_0. Considering that the behavior of the filaments is elastic prior to failure, the stress in the filaments is not induced uniformly and depends on the filament direction (inclination). An appropriate magnitude of the stress to be used in model predictions is an average stress in filament segments subjected to extension at the instant of composite failure. A sound estimate of this average stress can be made, since, as shown consistently by all laboratory tests, the composite fails at a reasonably well-defined strain.

The average strain of the polyester filament at failure was reported by Sanvito (1995) as 21 or 23% at the strain rate of 100 and 10 mm/min, respectively. The failure of the reinforced specimens occurred at the axial strain of about 7–10% (depending on the confining pressure and the sand used, the smaller strain is for low confining pressure). To estimate the strength mobilization in the filaments we first introduce the dilatancy angle ν in triaxial compression as

$$\frac{\dot{\varepsilon}_1 + \dot{\varepsilon}_2 + \dot{\varepsilon}_3}{\dot{\varepsilon}_1 - \dot{\varepsilon}_2 - \dot{\varepsilon}_3} = -\sin \nu \tag{35}$$

The expression in (35) was derived assuming the nonassociative flow rule and the plastic potential in a form identical to the Mohr-Coulomb function, but with the internal friction angle replaced by dilatancy angle ν. Since in triaxial compression $\dot{\varepsilon}_1 > \dot{\varepsilon}_2 = \dot{\varepsilon}_3$, the relation between $\dot{\varepsilon}_1$ and $\dot{\varepsilon}_3$ following from (35) is

$$\frac{\dot{\varepsilon}_3}{\dot{\varepsilon}_1} = -\frac{1}{2}\,K \tag{36}$$

where

$$K = \frac{1 + \sin \nu}{1 - \sin \nu} = \tan^2\left(\frac{\pi}{4} + \frac{\nu}{2}\right) \tag{37}$$

Thus for an incompressible composite ($\nu = 0$) subjected to triaxial compression, the maximum extension rate in the filaments during composite failure is exactly half of the axial strain rate, and it increases with an increase in the dilation angle. To estimate the strength mobilized in the filaments, we assume that the ratio of the total strains at failure is the same as the ratio of their rates (36). The dilation angles for the reinforced composite reported by di Prisco and Nova (1993) and Sanvito (1995) are only a few degrees, and calculations were performed for $\nu = 0$ and $\nu = 5°$.

Considering that the axial composite strain (ε_1) at failure is about 10%, the maximum extension of the filaments (ε_3) at failure is only 5% for an incompressible composite and 5.95% for a composite with dilation angle $\nu = 5°$. Moreover, the filament strain is not uniform and reaches its maximum for portions of the filaments oriented in the ε_2, ε_3($\varepsilon_2 = \varepsilon_3$ in triaxial compression tests) plane. The weighted average of the extension strain in filaments can be estimated as

$$\bar{\varepsilon} = \frac{\int_V \rho(\theta)\varepsilon_\theta \, dV}{\int_V \rho(\theta) \, dV} \tag{38}$$

where volume V includes only fibers in the tensile regime, and ε_θ is the strain in filaments inclined at θ to the plane of max-

TABLE 1. Experimental Results from Triaxial Compression Tests and Model Prediction

Source (1)	Unreinforced Sand: φ (°) (2)	Filament: $\rho(\rho_w)$ (%) (3)	Filament: Tenacity (cN/tex) (4)	Filament: Linear density (dtex/filament number) (5)	Reinforced Sand: γ_d (kN/m^3) (6)	Reinforced Sand: φ (°) (7)	Reinforced Sand: Cohesion (kPa) (8)	Model Prediction: Cohesion ($\nu = 0$) (kPa) (9)	Model Prediction: Cohesion ($\nu = 5°$) (kPa) (10)
di Prisco and Nova (1993)	40	0.144 (0.142)	50	167/30	13.5	40	70	59.7	71.1
Stauffer and Holtz (1995)	40	0.233 (0.20)	36	167/30	16.1	44	83	95.9	115.1
Sanvito (1995)	35	0.234 (0.20)	38.5	78/24	15.5	37	135	84.6	101.6
Leflaive and Liausu (1986)	43	0.286 (0.20)	36	330/60	19.0	48	190	127.6	153.1

imum extension in the triaxial compression test. Taking function $\rho(\theta)$ in the form of (34), one obtains [from (38)] $\bar{\varepsilon} = 0.7$ of ε_3 for incompressible composite, and $\bar{\varepsilon} = 0.705$ when $\nu = 5°$. Consequently, the average extension strain of the filaments at failure is only 3.5 or 4.2% for $\nu = 0$ and $\nu = 5°$, respectively.

The initial elastic modulus of polyester thread was reported by di Prisco and Nova (1993) as being slightly over 10 GPa. If the behavior of the polyester is approximated as linear prior to failure, the deformation modulus would become 2–3 GPa. Mobilization of stress in filaments depends on the history of deformation, and any attempt to assess its magnitude without analysis of the process is bound to be approximate. We will assume in the calculations that the average stress in filaments at failure is proportional to the average strain at failure with the deformation modulus of 3 GPa.

Results from triaxial tests are given in the literature in terms of apparent cohesion. This is the maximum value of cohesion in the anisotropic composite, because in triaxial compression the horizontal bedding plane benefits the macroscopic strength most. Calculations then were performed using (32) and (33) (with $n = 2$ and $b = 0$), where $\psi = \pi/2$ and $\omega = 0$ [point A in Fig. 6(a); the magnitude of R at point A, calculated at $p = 0$, divided by $\cos\varphi$ yields the prediction of the maximum cohesion].

The comparison of the model prediction and results from laboratory tests are shown in Table 1. The internal friction angle of unreinforced sand is given in column 2, and the filament content by volume ρ (and by weight ρ_w) is shown in column 3. The internal friction angle of the composite and its cohesion tested are given in columns 7 and 8, and the prediction of the cohesion using the proposed model is shown in the last two columns for an incompressible material and for dilatancy angle $\nu = 5°$. The yield strength of the filaments (calculated based on the given tenacity) is about 500 MPa, but the actual stress in the filaments at the time of composite failure is considerably less. As discussed earlier, at the instant of composite failure the filament strain is about 4%, whereas the filament failure occurs at more than 20% of strain.

The model suggested overestimated the apparent cohesion in one case and underestimated it in the remaining three cases. However, the numbers are reasonable for the first theoretical estimate. The comparison of experimental results by Stauffer and Holtz (1995) and Sanvito (1995) is somewhat surprising: both have approximately the same content of filaments, the one with the lower internal friction angle of the matrix exhibits a significantly higher apparent cohesion. This suggests that it may not be feasible to seek a more accurate description of failure without including further micromechanics-based considerations (the two composites were reinforced with filaments of similar deformation modulus, but of significantly different length).

The experimental tests also suggest that the internal friction angle of the composite is larger than that of the granular matrix, whereas the model does not predict any increase. This is because the contribution of the filaments to the composite strength was included as a dissipation term independent of the composite stress state [compare with (33)]. The increase in the internal friction angle suggests that there may be some slippage of the filaments in the matrix during composite failure. The work dissipation rate in the slip regime is dependent on the stress in the composite, and including such terms in the model could account for the increase in internal friction.

It can be disputed whether triaxial tests can be used to verify the plane-strain model derived. The failure criterion (Mohr-Coulomb) and the normality flow rule used lead to a zero work dissipation rate in the matrix material, independent of whether its deformation is in-plane or axisymmetrical (the internal friction angle of the matrix sand used in predictions was determined through triaxial testing). However, different deformation modes affect theoretical results differently through the contribution of the filaments, but the difference here was not significant.

FINAL REMARKS

A model describing failure of granular soils reinforced with continuous filaments has been presented. The homogenization method was used in order to find the macroscopic stresses at failure. The mechanism of stress transfer from granular matrix to thin thread reinforcement is different from that in short fiber composites. The filaments form a dense network of reinforcement wrapped around clusters of grains, and the primary stress transfer mechanism is analogous to the increase of forces in a belt wrapped around a rigid drum (belt friction effect).

A polyester thread generally does not reach the yield point during the deformation process since the failure of the composite occurs at strains lower than that associated with filament failure. Rupture of filaments may occur locally, however, because some micromechanical thread-grain configurations may induce large strains locally in small portions of filaments. This phenomenon was not found significant enough to be included in the model.

The failure criterion derived was found to predict reasonable numbers, but the model can be improved through a more accurate account of the stress mobilization in the filaments at the instant of composite collapse, and by including a slip component of work dissipation during failure. Further studies also are needed on the micromechanics of the soil-filament interaction.

ACKNOWLEDGMENTS

The research presented in this paper was supported by the Air Force Office of Scientific Research, Grant No. F49620-1-0109, and by the National Science Foundation, Grant No. CMS9634193. This support is greatly appreciated.

APPENDIX I. ENERGY DISSIPATION RATE EXPRESSION

Considering the relation in (15), the expression in (21) can be written as

$$\dot{D}(\dot{\varepsilon}_{ij}) = \frac{1}{\pi}\sigma_0\dot{\varepsilon}_1 \int_S \rho(\theta)\frac{1}{R_0^2}\left(K_p\frac{x^2}{R_0^2} - \frac{y^2}{R_0^2}\right) dS \qquad (39)$$

From the geometrical relations in Fig. 3(a) [or Fig. 4(c)] we have: $y/R_0 = \sin\theta$, $x/R_0 = \cos\alpha\cos\theta$, $dS = R_0^2\cos\theta\, d\alpha\, d\theta$, and (39) can be transformed into

$$\dot{D}(\dot{\varepsilon}_{ij}) = \frac{1}{\pi}\sigma_0\dot{\varepsilon}_1 \int_0^{\pi/2}\int_{-\theta^*}^{\theta^*} \rho(\theta)(K_p\cos^2\alpha\cos^2\theta - \sin^2\theta)\cos\theta\, d\theta\, d\alpha \qquad (40)$$

Since the distribution of the filaments is axisymmetrical and the deformation is plane, the integration limits on θ, which include all filaments in the tensile regime $(-\theta^*, \theta^*)$, depend on angle α [see Fig. 4(c)]. From geometrical relations it follows that

$$\theta^* = \arctan(\cos\alpha\tan\theta_0) \qquad (41)$$

where θ_0 is expressed in (23).

APPENDIX II. REFERENCES

Budiansky, B. (1965). "On the elastic moduli of some heterogeneous materials." *J. Mech. Phys. Solids*, 13, 223–227.

Davis, E. H. (1968). "Theories of plasticity and the failure of soil masses." *Soil mechanics: selected topics*, I. K. Lee, ed., Butterworth's London, U.K., 341–380.

di Prisco, C., and Nova, R. (1993). "A constitutive model for soil reinforced by continuous threads." *Geotextiles and Geomembranes*, 12, 161–178.

Hashin, Z. (1983). "Analysis of composite materials—a survey." *J. Appl. Mech., Trans ASME*, 50, 481–505.

Hill, R. (1965). "A self-consistent mechanics of composite materials." *J. Mech. Phys. Solids*, 13, 213–222.

Khay, M., Gigan, J. P., and Ledelliou, M. (1990). "Reinforcement with continuous thread: technical developments and design methods." *Proc., 4th Int. Conf. Geotextile Geomembrane Related Products, Vol. 1*, A. A. Balkema, Rotterdam, The Netherlands, 21–26.

Leflaive, E., and Liausu, P. (1986). "The reinforcement of soils by continuous threads." *Proc., 3rd Int. Conf. on Geotextiles, Vol. 4*, Gisteldruck, Vienna, Austria, 1159–1162.

McLaughlin, P. V., and Batterman, S. C. (1970). "Limit behavior of fibrous materials." *Int. J. Solids Struct.*, 6, 1357–1376.

Michalowski, R. L., and Zhao, A. (1995). "Continuum versus structural approach to stability of reinforced soil." *J. Geotech. Engrg.*, ASCE, 121(2), 152–162.

Michalowski, R. L., and Zhao, A. (1996a). "Failure of fiber-reinforced granular soils." *J. Geotech. Engrg.*, ASCE, 122(3), 226–234.

Michalowski, R. L., and Zhao, A. (1996b). "Failure of unidirectionally reinforced composites with frictional matrix." *J. Engrg. Mech.*, ASCE, 122(11), 1086–1092.

Sanvito, E. (1995). "Analisi sperimentale numerica di campioni di sabbia rinforzata con filo continuo," PhD dissertation, Politecnico di Milano, Italy.

Shu, L. S., and Rosen, B. W. (1967). "Strength of fiber-reinforced composites by limit analysis methods." *J. Comp. Mat.*, 366–381.

Stauffer, S. D., and Holtz, R. D. (1995). "Stress-strain and strength behavior of staple fiber and continuous filament-reinforced sand." *Transp. Res. Rec. 1474*, Transp. Res. Board, Washington, D.C., 82–95.

Villard, P., and Jouve, P. (1989). "Behaviour of granular materials reinforced by continuous threads." *Comp. and Geotech.*, 7, 83–98.